Received: 28 September 2018 | Revised: 18 November 2018 | Accepted: 1 February 2019
DOI: 10.1002/aoc.4882

FULL PAPER

WILEY Applied Organometallic Chemistry

Spectral and crystallography studies of new palladacycle complexes with P,C- and C,C-donor ligands; Application of (OAL16) to optimizing the yield of Mizoroki-Heck reaction

Seyyed Javad Sabounchei[1] | Khadijeh Badpa[1] | Ali Hashemi[1] | Faezeh Moniriyan[1] |
Robert W. Gable[2]

[1] Faculty of Chemistry, Bu-Ali Sina University, Hamedan 65174, Iran

[2] School of Chemistry, University of Melbourne, Victoria 3010, Australia

Correspondence
Seyyed Javad Sabounchei, Faculty of Chemistry, Bu-Ali Sina University, Hamedan, 65174, Iran.
Email: jsabounchei@yahoo.co.uk

The new symmetrical diphosphonium salt $[Ph_2P(CH_2)_2PPh_2(CH_2C(O)C_6H_4Br)_2]$ Br_2 (**S**) was synthesized in the reaction of 1,2-bis(diphenylphosphino) ethane (dppe) and related ketone. Further treatment with NEt_3 gave the symmetrical α-keto stabilized diphosphine ylide $[Ph_2P(CH_2)_2PPh_2(CHC(O)C_6H_4Br)_2]$ (**Y^1**). The unsymmetrical α-keto stabilized diphosphine ylide $[Ph_2P(CH_2)_2PPh_2(CHC(O)C_6H_4Br)]$ (**Y^2**) was synthesized in the reaction of diphosphine in 1:1 ratio with 2.3′-dibromoacetophenone, then treatment with $NEt_{3.}$ The reaction of dibromo (1,5-cyclooctadiene)palladium (II), $[PdBr_2(COD)]$ with this ligand (**Y^1**) in equimolar ratio gave the new C,C-chelated $[PdBr_2(Ph_2P(CH_2)_2PPh_2(C(H)C(O)C_6H_4Br)_2)]$ (**1**) and with unsymmetrical phosphorus ylide $[Ph_2P(CH_2)_2PPh_2C(H)C(O)C_6H_4Br]$ (**Y^2**) gave the new P, C-chelated palladacycle complex $[PdBr_2(Ph_2P(CH_2)_2PPh_2C(H)C(O)Br)]$ (**2**). These compounds were characterized successfully by FT-IR, NMR (^1H, ^{13}C and ^{31}P) spectroscopic methods and the crystal structure of **Y^1** and **2** were elucidated by single crystal X-ray diffraction. The results indicated that the complex **1** was C, C-chelated whereas complex **2** was P, C-chelated. These air/moisture stable complexes were employed as efficient catalysts for the Mizoroki-Heck cross-coupling reaction of several aryl chlorides, and the Taguchi method was used to optimize the yield of Mizoroki-Heck coupling. The optimum condition was found to be as followed: base; K_2CO_3, solvent; DMF and loading of catalyst; 0.005 mmol.

KEYWORDS
Pd -cyclic complexes, phosphorus ylide, symmetrical phosphorus ylide, Taguchi method, unsymmetrical X-ray

1 | INTRODUCTION

Stabilized phosphorus ylides derived from diphosphines are important reagents in organic chemistry, and have shown more useful application in organometallic chemistry due to their ambidentate character as ligands.[1–3] Furthermore, they are valuable key intermediates in metal-mediated organic synthesis.[4,5] Also, the basicity or steric properties of the two phosphorus atoms in these phosphorus ylides can be different and may be used to get different coordination modes.[6] The coordination chemistry of α-keto stabilized phosphorus ylides is interesting to chemists, because of the different bonding modes upon coordination of ylides to metal,[7–10] a) C-coordinated (through the Cα atom), b) O- coordinated (through the O atom of the carbonyl), c) P- coordinated (through the P atom of the phosphine group), and d) even situations in which the same ylide shows a combination of bonding modes (Scheme 1).

Additionally, Pd (II) complexes bearing phosphine groups have been extensively applied as efficient catalysts in some cross-coupling reactions,[11–17] specifically, the Mizoroki-Heck reaction. The Mizoroki-Heck reaction, has emerged as the most important and reliable method for construction of functionalized olefins, and it can be catalyzed with the Pd (II) complexes of such phosphorus ylides.[18,19] Palladium complexes (**1** and **2**) were employed as homogeneous catalysts in C-C coupling reactions. There are many controlling factors such as base, solvent, temperature, time, catalyst (mol%), etc. The appropriate selection of conditions for cross coupling reactions can be done with the Taguchi Method. The Taguchi method is generally used for process optimization, because it can noticeably reduce the time and costs associated with achieving optimum conditions.[20] Therefore, some of the possible analytical methods like Taguchi, analysis of variance (ANOVA), and signal-to-noise (S/N) ratio were used in this work.

In this work we have focused our attention to the synthesis, spectroscopic (IR and NMR) and X-ray structural characterization of these new complexes of phosphorus ylide. Furthermore Pd (II) complex catalyzed Mizoroki-Heck coupling reaction of various aryl chlorides and olefins is reported.

2 | EXPERIMENTAL

2.1 | Materials and methods

All synthetic reactions were carried out under dry nitrogen using standard Schlenk techniques. 2-bromo-3′-bromoacetophenone, (1,5-cyclooctadiene) (COD) and 1,2-bis (diphenylphosphino) ethane dppe were purchased from commercial sources and used without further purification. The [$PdBr_2$(COD)] complex was prepared according to previously published procedures.[21] Phosphorus ylide Y^2 was synthesized and characterized with previously published method.[3] Toluene, n-hexane and chloroform were used as reagent grade and dried over Na/Benzophenone and $CaCl_2$ subsequently. The ^{1}H, ^{13}C and ^{31}P NMR spectra were recorded on 250 MHz Bruker and 90 MHz Jeol spectrometers with $CDCl_3$ as solvent at 25 °C. IR spectra were recorded with KBr pellets using a Shimadzu 435-U04 spectrophotometer in the region of 4000–400 cm^{-1}.

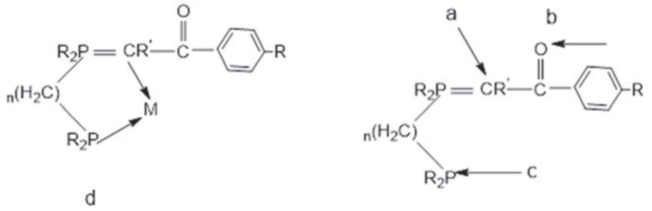

SCHEME 1 The possible coordination modes of phosphine ligands

2.2 | Synthesis of diphosphonium salt

2.2.1 | General procedure

A solution consisting of 1, 2-bis (diphenylphosphino) ethane (0.25 mmol) and ketone (0.5 mmol) in acetone (5 ml) was stirred at room temperature for 24 hr. The resulting solution was filtered off and concentrated to *ca.* 3 ml under reduced pressure and then treated with diethyl ether to precipitate the diphosphonium salt.

2.2.2 | Data for $[Ph_2P(CH_2)_2PPh_2(CH_2C(O)C_6H_4Br)_2]\ Br_2$ (S)

Yield*:* 0.051 g (85%), M.p. 212 °C. IR (KBr disk) ν (cm^{-1}): 1669(C=O). ^{1}H NMR ($CDCl_3$) δ_H (ppm): 4.04 (br, 4H, CH_2), 6.06 (br, 2H, PCH2CO); 7.58–8.28 (m, 28H, Ph). ^{31}P NMR ($CDCl_3$) δ_P (ppm): 26.76 (s, PCH_2). ^{13}C NMR ($CDCl_3$) δ_C (ppm): 15.29(m, CH_2); 32.9 (m, PCH_2); 116.95–137.9 (m, Ph); 191.9 (s, CO).

2.3 | Synthesis of diphosphine ylide

2.3.1 | General procedure

The diphosphonium salt was further treated with triethyl amine (0.5 ml) in dry toluene. The triethylammonium bromide was filtered off. Concentration of the toluene layer to *ca.* 3 ml and subsequent addition of petroleum ether (20 ml) resulted in the precipitation of diphosphine ylide.

2.3.2 | Data for $[Ph_2P(CH_2)_2PPh_2(CHC(O)C_6H_4Br)_2]$ (Y^1)

Yield*:* 0.051 g (85%), M.p. 212 °C. Anal. Calcd. for $C_{42}H_{34}Br_2O_2P_2$ (%): C, 63.66; H, 4.32. Found: C, 63.75; H, 4.43. IR (KBr disk) ν (cm^{-1}): 1568(C=O). ^{1}H NMR ($CDCl_3$) δ_H (ppm): 3.33 (s, 4H, CH_2); 4.24 (m, 1H, PCH); 7.24–8.16 (m, 28H, Ph).^{31}P NMR ($CDCl_3$) δ_P (ppm): 15.26 (s). ^{13}C NMR ($CDCl_3$) δ_C (ppm): 18.81(m, CH_2); 47.9(m, PCH); 122.33–143.17 (m, Ph); 183.46 (s, CO).

2.4 | Synthesis of Pd complexes

2.4.1 | General procedure

To a dichloromethane solution of [$PdBr_2$(COD)] (0.5 mmol, 5 ml), a solution of ylide (0.5 mmol) (5 ml, CH_2Cl_2) was added. The resulting solution was stirred for 2 hr at room temperature and then concentrated to a *ca*. 2 ml under reduced pressure and treated with n-hexane (5 ml) to afford a yellow precipitate of the Pd complexes of the desired diphosphine ylide.

2.4.2 | Data for [$PdBr_2$(Ph_2P(CH_2)$_2$$PPh_2$(C(H)C(O)$C_6H_4$-*m*-Br)$_2$)] (1)

Yield: 0.054 g (95%), M.p. 205 °C. IR (KBr disk) ν (cm^{-1}): 1634 (C=O). ^{1}H NMR ($CDCl_3$) δ_H (ppm): 3.7 (m, 4H, PCH_2); 6.5 (br, 1H, PCH); 7–8.6 (m, 28H, Ph). ^{31}P NMR ($CDCl_3$) δ_P (ppm): 29.57 (d, PPh_2, $^2J_{P\text{-}P}$ = 4 Hz); 32.9 (d, PCH, $^2J_{P\text{-}P}$ = 4 Hz). ^{13}C NMR ($CDCl_3$) δ_C (ppm): 38.72(s, CH_2); 50.81 (s, PCH); 118.78–140.87 (m, Ph); 197.99(s, CO).

2.4.3 | Data for [$PdBr_2$(Ph_2P(CH_2)$_2$$PPh_2$C(H)C(O)$C_6H_4$-*m*-Br)] (2)

Yield: 0.051 g (85%), M.p. 212 °C. Anal. Calcd. for $C_{34}H_{29}Br_3OP_2Pd$ (%): C, 52.15; H, 5.53. Found: C, 52.23; H, 5.64. IR (KBr disk) ν (cm^{-1}): 1622(C=O). ^{1}H NMR ($CDCl_3$) δ_H (ppm): 4.8 (m, 4H, PCH_2P); 5.8 (s, H, PCH); 7–8.3 (m, 24H, Ph).^{31}P NMR ($CDCl_3$) δ_P (ppm): 22.54 (d, PPh_2, $^2J_{P\text{-}P}$ = 22.22 Hz); 30.66 (d, PCH, $^2J_{P\text{-}P}$ = 22.22 Hz). ^{13}C NMR ($CDCl_3$) δ_C (ppm): 27.94(s, CH_2); 49 (s, PCH); 121.81–140.32 (m, Ph); 194.25(s, CO).

2.5 | Crystallography

Single crystals of **Y^1** and **2** were crystallized by slow evaporation from dichloromethane solution. A suitable crystal was selected and mounted on a Rigaku Oxford Diffraction SuperNova, Dual, Cu at zero, Atlas diffractometer. The crystal was kept at 130.00(10) K during data collection. Using Olex2,[22] the structure was solved with the ShelXT[23] structure solution program using Intrinsic Phasing and refined with the ShelXL[24] refinement package using Least Squares minimization. Gaussian absorption corrections were applied to the data. All non-hydrogen atoms were refined with anisotropic displacement parameters, using all data. Hydrogen atoms were located in ideal positions. For 2 there were two independent molecules in the asymmetric unit, together with a molecule of dichloromethane and a partially occupied molecule of solvent water; the occupancy factor refined to 0.368(13) (See supporting information).

2.6 | Typical procedure for the Mizoroki-heck reaction

2.6.1 | General procedure

Palladium (II) complex **2** (0.005 mmol), olefin (0.75 mmol), aryl chloride (0.5 mmol), K_2CO_3 (1 mmol) and DMF (2 ml) were added to a small tube and the mixture was heated to 130 °C for 6 hr in the presence of air. The reactions were monitored by thin-layer chromatography (TLC). After being cooled to ambient temperature, the mixture was extracted with n-hexane: EtOAc (8:2) filtered and purified by recrystallization from ethanol and water or purified by silica gel column chromatography to give a crude product which was analyzed by ^{1}H and ^{13}C NMR spectroscopy.

2.6.2 | Data for *p*-CH_3-Ph-CH=CHCOOEt (5a)

^{1}H NMR ($CDCl_3$) δ_H (ppm): δ = 7.66 (d, 1H, CHCO, J = 16.21 Hz), 7.13–7.47 (m, 4H, Ph), 6.38 (d, 1H, CHPh J = 16.03 Hz), 4.26 (q, 2H, CH_2, J = 7.07 Hz), 2.37 (s, 3H, CH_3), 1.33 (t, 3H, CH_3 J = 6.98 Hz). ^{13}C NMR (ppm): δ = 167.2 (s, CO), 144.5, 140.6, 131.7, 129.6, 128.0, 117.1, 60.4 (s, CH_2), 21.4 (s, CH_3), 14.3 (s, CH_3).

2.6.3 | Data for *p*-CHO-Ph-CH=CHCOOEt (5b)

^{1}H NMR ($CDCl_3$) δ_H (ppm): 9.95 (s, 1H, CHCO), 7.35–7.88 (m, 5H, Ph), 6.47 (d, 1H, CHPh, J = 16.21 Hz), 4.23 (q, 2H, CH_2, J = 7.25 Hz), 1.28 (t, 3H, CH_3, J = 6.98 Hz). ^{13}C NMR (ppm): δ = 190.4 (s, CO), 165.3 (s, CO), 141.7, 139.0, 136.0, 129.1, 127.4, 120.3, 59.7 (s, CH_2), 13.2 (s, CH_3).

2.6.4 | Data for *p*-NO_2-Ph-CH=CHCOOEt (5c)

^{1}H NMR ($CDCl_3$) δ_H (ppm): 7.18–8.22 (m, 5H, Ph), 6.47 (d, 1H, CHCO, J = 16.03 Hz), 4.22 (q, 2H, CH_2, J = 7.07 Hz), 1.28 (t, 3H, CH_3, J = 7.34 Hz). ^{13}C NMR (ppm): δ = 166.7 (s, CO), 139.5, 137.0, 130.8, 128.3, 128.0, 117.0, 60.4 (s, CH_2), 14.3 (s, CH_3).

2.6.5 | Data for Ph-CH=CHCOOEt (5d)

^{1}H NMR (CDCl$_3$) δ_H (ppm):7.56 (d, 1H, CHCO, J = 16.10 Hz), 7.24–7.65 (m, 5H, Ph), 6.30 (d, 1H, CHPh, J = 16.03 Hz), 4.13 (q, 2H, CH$_2$, J = 6.98 Hz), 1.20 (t, 3H, CH$_3$, J = 6.98 Hz). ^{13}C NMR (ppm): δ = 165.8 (s, CO), 143.4, 133.3, 129.1, 127.8, 126.9, 117.1, 59.3 (s, CH$_2$), 13.2 (s, CH$_3$).

2.6.6 | Data for *p*-CH$_3$OC-Ph-CH=CHCOOEt (5e)

^{1}H NMR (CDCl$_3$) δ_H (ppm):7.77 (d, 1H, CHCO, J = 15.68 Hz), 6.99–7.37 (m, 4H, ph), 6.22 (d, 1H, CHPh, J = 15.77 Hz), 4.23 (q, 2H, CH$_2$, J = 7.07 Hz), 2.56 (s, 3H, CH$_3$), 1.31 (t, 3H, CH$_3$O, J = 7.16 Hz). ^{13}C NMR (ppm): δ = 197.2 (s, CO), 166.7 (s, CO), 138.5, 137.0, 130.8, 128.3, 128.1, 117.0, 60.6 (s, CH$_2$), 14.2 (s, CH$_3$).

3 | RESULTS AND DISCUSSION

3.1 | Synthesis

Diphosphine Ph$_2$P(CH$_2$)$_2$PPh$_2$ reacts in 1:2 ratio with 2.3′-dibromoacetophenone forming the new diphosphonium salt **S** in 90–95% yields. Further treatment of this salt with triethyl amine leads to elimination of HBr, giving the new symmetrical diphosphine ylide **Y^1** in 80–85% yields. The reaction of [PdBr$_2$(COD)] with this ligand (**Y^1**) in equimolar ratio gave the new C,C-chelated [PdBr$_2$(Ph$_2$P(CH$_2$)$_2$PPh$_2$(C(H)C(O)C$_6$H$_4$Br)$_2$)] (**1**) and with the unsymmetrical phosphorus ylide [Ph$_2$P(CH$_2$)$_2$PPh$_2$C(H)C(O)C$_6$H$_4$Br] (**Y^2**) gave the P, C-chelated palladacycle complex [PdBr$_2$(Ph$_2$P(CH$_2$)$_2$PPh$_2$C(H)C(O)Br)] (**2**) (Scheme 2). All complexes are moderately soluble in dichloromethane and insoluble in non-polar solvents, such as n-hexane.

3.2 | Characterization

The structure of products was characterized by IR, ^{1}H, ^{13}C and ^{31}P NMR spectroscopic methods; Table 1 shows important details.

3.2.1 | Infra-red spectra

The ν (CO) in the IR spectra of phosphorus ylide **Y^1** was observed in lower frequencies than those of the related phosphonium salt **S**, suggesting some lowering of electron density in the C=O bond. As noted in the literature,[25] coordination of ylide through the carbon, causes a significant increase in the ν CO frequency. IR spectra of complexes **1** and **2** show a significantly frequency shift of ν (CO) than those of the related phosphorus ylides **Y^1** and **Y^2**. These observations are in agreement with the chelating of ylide **Y^1** through two Cα atoms and ylide **Y^2** through the P and Cα atoms. Presence of ν CO bands around 1634–1622 cm^{-1} in the IR spectra of these complexes indicates that products (C, C and P, C-chelated complexes) were formed.

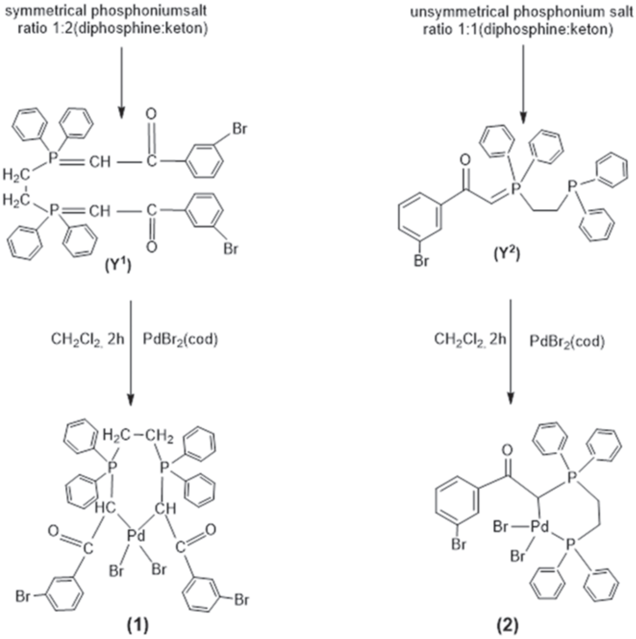

SCHEME 2 Synthesis of palladacycle complexes 1, 2

TABLE 1 Spectroscopic data for compounds **S**, **Y^1**, **Y^2**, **1** and **2**

Compound	IR; ν (CO) cm^{-1}	^{1}H NMR; δ (PCHor PCH$_2$) ppm	^{13}C NMR; δ (CO) ppm	^{31}P NMR; δ (PCH) and (PPh$_2$) ppm
S	1669	6.06	191.9	26.76
Y^1	1568	4.24	183.46	15.26
Y^2	1571	4.08	183.36	14.45, −15.63
1	1634	6.33	197.99	32.9, 29.57
2	1622	6.41	194.25	30.66, 22.54

3.2.2 | NMR

The ^{31}P NMR spectra of phosphonium salt **S** shows a singlet around 26.76 ppm, due to the PPh$_2$ groups, which indicates that the two phosphorus atoms are equivalent, this peak shifted to around 15.26 ppm in spectra of ylide

Y^1, and show upfield shift compared to that of parent phosphonium salt, suggesting some electron density increase in the P–C bond. The ^{31}P chemical shift values for complexes **1** and **2** appear to be shifted downfield with respect to parent ylides **Y^1** and **Y^2**, indicating that coordination of the ylide has occurred. Coordination of phosphorus ylides as C, C-chelated and P, C-chelated forms can make a large chemical shift for both free (PPh$_2$) and bonded (PCH) phosphorus atoms. While, in P, P- coordinated form only the signal of PPh$_2$ moiety was shifted to higher frequencies. The ^{31}P NMR spectrum of the complex **1** features two doublets around 29.57, 32.9 ppm, shifted downfield compared with that of the phosphorus ylide (around 15.26 ppm), due to the coordination of the ylide to palladium through the carbon atoms (ylidic carbon).[26] The ^{31}P NMR spectrum of complex **2** shows two doublet peaks around $\delta = 22.54$, 30.66 ppm which are assigned to PPh$_2$ and PCH, respectively.

The ^{1}H NMR spectra of the ylide **Y^1** shows an upfield shift in the CH signals compared to those of the phosphonium salt **S**. These observations were related to the increasing of the electron density in the P-C bonds. The ^{1}H NMR spectra of complexes **1** and **2** exhibit characteristic shifts in the methinic proton signals. This is interesting, because complexation of the ylides **(Y^1/Y^2)** to Pd through free phosphorus atom did not significantly change the chemical shift values of ^{1}H NMR. While, coordination through carbanion causes to shift of PCH peaks to higher frequency around 6.33–6.41 ppm. The ^{1}H chemical shift values for these complexes appeared to be shifted downfield with respect to the parent ylide, indicating also that the coordination of the ylide **Y^1** in complex **1** has occurred through two Cα atoms and in complex **2** of the ylide **Y^2** through P and Cα atoms.

In the ^{13}C NMR spectra of complexes **1** and **2**, most of the expected resonances are visible and characteristic peaks of carbonyl, methinic and methanediyl groups in complexes **1** and **2** show downfield shift respect to the parent ylide **Y^1** and **Y^2**. Furthermore, strong deshielding in resonance value was observed for the CH$_2$ after complexation (around *10* ppm), which is in agreement with the C,C- coordination character of the ylide in complex **1**. These observations also confirmed that coordination of ylides **Y^2** has occurred through P and Cα atoms and ylide **Y^1** has occurred through the two Cα atoms.

3.3 | Crystallography

Suitable single crystals of **Y^1** and **2** were grown by slow evaporation from dichloromethane solution. The molecular structures of **Y^1** and **2** are shown in Figure 1 and Figure 2, respectively. Relevant parameters concerning data collection and refinement are given in Table 2. Selected bond distances and angles for the unit cells of **Y^1** and **2** are displayed in Table 3.

3.3.1 | Crystal structures of Y^1

The molecule lies on a center of symmetry. The phosphorous atom is coplanar with the keto group, the dihedral angle between these atoms and the aromatic ring is 21.08(9)° while the Br atom on the attached aromatic ring is oriented away from the carbonyl oxygen, the Br$_1$-C$_5$ ...

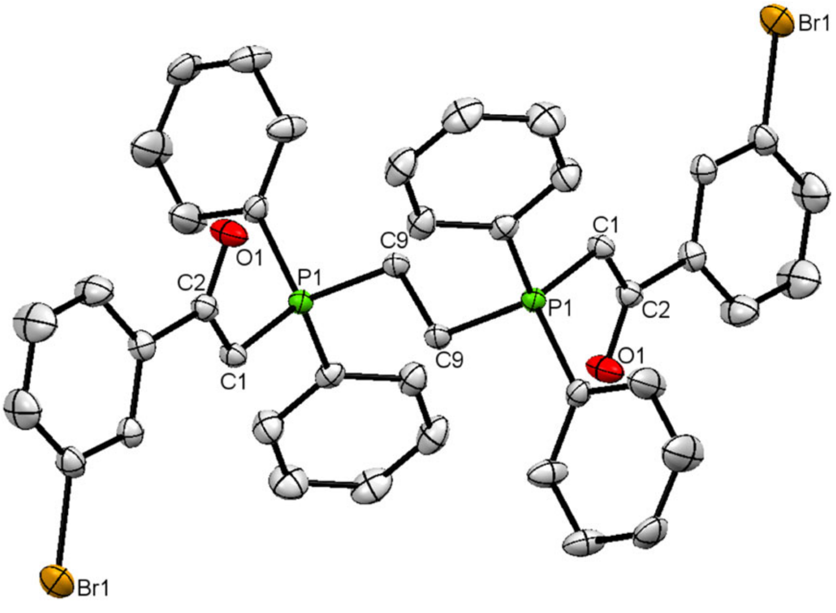

FIGURE 1 ORTEP view of X-ray crystal structure Y1

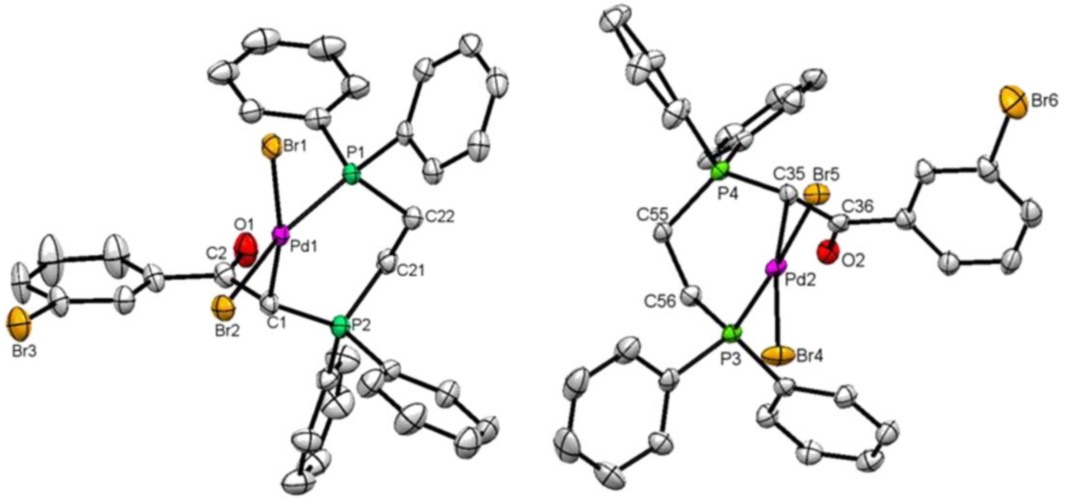

FIGURE 2 ORTEP view of X-ray crystal structure of molecules 1 and 2

C_2-O_1 torsion angle being −154.77(16)°. The structure has some similarities to 2,2′-(ethane-1,2-diylbis(diphenylphosphoranylylidene))bis(1-(2,4-dichlorophenyl)ethanone),[12] in particular the observation that the P_1-C_1 and C_1–C_2 bond lengths are shorter than the normal values found for (P^+–C (sp^3)) and (C–C (sp^3)) bonds, 1.800 Å and 1.511 Å, respectively,[27] while the C-O bond length is significantly longer than the normal value of 1.210 Å. This has been attributed to the ylidic resonance involving electron delocalization over the P_1-C_1–C_2–O_1 moiety.[12,27] One main difference between the two structures, however, is that the dihedral

TABLE 2 Crystal data and structure refinement for **Y^1** and **2**

	Compound Y^1	**Compound 2**
Empirical formula	$C_{42}H_{34}O_2P_2Br_2$	$C_{69}H_{60.74}Br_6Cl_2O_{2.37}P_4Pd_2$
Formula weight	792.45	1814.83
T [K]	130.00(10)	130.00(10)
Crystal system	orthorhombic	monoclinic
Space group	Pbca	$P2_1/c$
a [Å]	15.72121(12)	21.2364(2)
b [Å]	8.79483(9)	19.1159(2)
c [Å]	25.5658(2)	16.81993(16)
α [°]	90	90
β [°]	90	99.6027(10)
γ [°]	90	90
V [Å^3]	3534.86(6)	6732.43(13)
Z	4	4
ρ_{calc}g/cm^3	1.489	1.790
μ [mm $^{-1}$]	4.047	10.467
F(000)	1608.0	3558.7
2θ range [°]	6.91 to 154.23	7.056 to 154.232
Index ranges	$-11 \le h \le 19$, $-11 \le k \le 10$, $-31 \le l \le 32$	$-26 \le h \le 23$, $-18 \le k \le 24$, $-20 \le l \le 21$
Independent reflections	3733 [$R_{int} = 0.0282$, $R_{sigma} = 0.0121$]	14063 [$R_{int} = 0.0437$, $R_{sigma} = 0.0370$]
Data/restr./param.	3733/0/218	14063/4/782
Goodness-of-fit on F^2	1.031	1.055
R_1/wR_2[$I > 2\sigma(I)$]	$R_1 = 0.0286$, w$R_2 = 0.0710$	$R_1 = 0.0452$, w$R_2 = 0.1242$

TABLE 3 Selected bond lengths [Å] and bond angles [°] for $\mathbf{Y^1}$ and **2**

		Compound 2			
Compound Y^1		**Mol 1**	**Mol 2**		
Bond distances					
$Br_1–C_5$	1.9042(19)	Pd_1-Br_1	2.4796(5)	Pd_2-Br_4	2.4675(5)
$O_1–C_2$	1.260(2)	Pd_1-Br_2	2.5056(5)	Pd_2-Br_5	2.4923(5)
$C_1–C_2$	1.396(2)	Pd_1-P_1	2.2321(10)	Pd_2-P_3	2.2500(10)
P_1-C_1	1.7203(15)	Pd_1-C_1	2.139(4)	Pd_2-C_{35}	2.122(4)
P_1-C_9	1.8148(16)	O_1-C_2	1.227(6)	O_2-C_{36}	1.228(5)
P_1-C_{10}	1.8071(16)	C_1-C_2	1.497(6)	C_{35}-C_{36}	1.485(6)
P_1-C_{16}	1.8090(16)	P_2-C_{21}	1.806(4)	P_4-C_{55}	1.806(4)
C_9-C_{9i}	1.528(3)	P_1-C_{29}	1.795(4)	P_3-C_{63}	1.808(4)
Bond angles					
$C_1–P_1–C_9$	113.41(7)	Br_2-Pd_1-Br_1	90.076(17)	Br_4-Pd_2-Br_5	90.640(16)
$C_2–C_1–P_1$	114.90(12)	C_1-Pd_1-P_1	95.88(11)	C_{35}-Pd_2-P_3	93.76(11)
$O_1–C_2–C_1$	122.17(15)	C_1-Pd_1-Br_1	167.42(12)	C_{35}-Pd_2-Br_4	171.44(11)
$C_4–C_5–Br_1$	117.95(14)	P_1-Pd_1-Br_1	86.57(3)	P_3-Pd_2-Br_4	87.78(3)
P_1-C_9-C_{9i}	111.25(14)	P_1-Pd_1-Br_2	166.06(3)	P_3-Pd_2-Br_5	175.27(3)

Symmetry Code: i 1-x,1-y,1-z

angle between the keto group and the attached chlorinated aromatic ring in this latter compound is 59.9° for molecule **1** and 61.9° for molecule **2**.

The carbonyl oxygen is involved in two weak C-H...O hydrogen bonds, an intramolecular interaction between the carbonyl oxygen and a methylene H-atom, and an intermolecular C-H...O interaction that links the molecules into a chain lying along the b-axis.

3.3.2 | Crystal structures of 2

There are two crystallographically independent molecules in the asymmetric unit. For molecule **2–1** the Pd is in a slightly tetrahedrally distorted square planar environment, comprising two cis-coordinating Br atoms, one phosphorous atom and an ylid carbon; the rms deviation of the four coordinating atoms, for molecule **2–1** is 0.260 Å, with Pd_1 lying 0.0094(13) Å out of the least squares plane. The keto oxygen is oriented away from the Pd atom, the torsion angle Pd_1 - C_1 - C_2 - O_1 being 99.4(4)°, while the dihedral angle between the bromo-substituted aromatic ring and the keto group is 7.3(4)°. For molecule **2–2** the distortion from ideal square planar geometry is somewhat greater; the rms deviation of the four coordinating atoms is 0.415 Å, with Pd_2 lying 0.1697(9) Å out of the least squares plane. The keto oxygen is oriented away from the Pd atom, the torsion angle Pd_2 - C_{35} - C_{36} - O_2 being 96.9(4)°, while the dihedral angle between the bromo-substituted aromatic ring and the keto group is 23.1(2)°. The main difference between the two molecules is in the conformation of the six-membered palladacycle rings. For molecule **2–1**, the ring is in a chair conformation (P_1, C_{22}, P_2, C_1 lying in the equatorial plane, with the rms deviation being 0.005 Å, and with Pd_1 and C_{21} in the axial positions), while for molecule **2–2**, the ring is in a highly distorted boat conformation (Pd_2, P_4, C_{55}, P_3 lying in the equatorial plane, with the rms deviation being 0.281 Å, and with C_{35} and C_{56} in the axial positions).

Both molecules show weak intermolecular and intramolecular and C-H ... O and C-H ... Br hydrogen bonds, the intermolecular C-H ... Br hydrogen bonds link the molecules along the c-axis (see Figure 3).

3.4 | Catalytic activity

3.4.1 | Optimization of reaction using Taguchi method

The catalytic activity of complexes **1** and **2** in the Mizoroki-Heck coupling reaction of aryl chlorides with ethyl acrylate was examined. The Taguchi method is a statistical approach to optimize the process parameters and can be expanded to improve the performance of total quality control[28] and involves identification of the appropriate control factors to obtain the optimum results

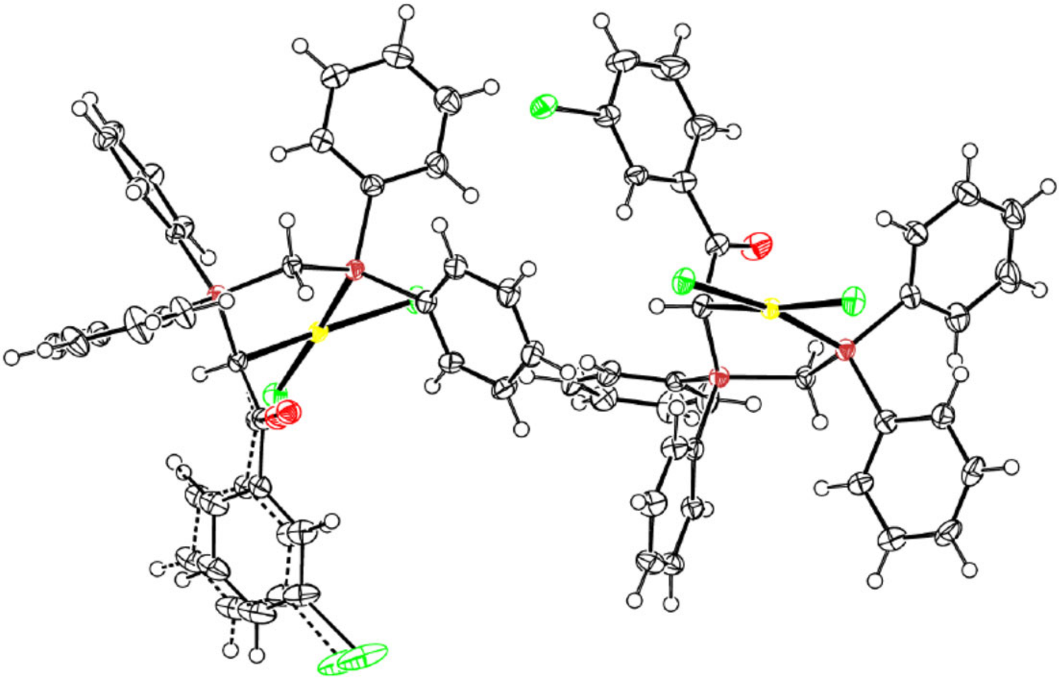

FIGURE 3 Intramolecular interaction between of the molecules 2–1 and 2–2

of the process. Initially, we set up a systematic optimization of reaction conditions using the Taguchi L16 experimental design. Orthogonal Arrays (OA) are used to conduct a set of experiments. In this work, the orthogonal array (OA), signal-to-noise ratio and the analysis of variance are employed to study the performance characteristics on response.[29] To select an appropriate orthogonal array for conducting the experiments, the degrees of freedom are to be computed. The three selected factors, including the base (B), solvent (S) and catalyst loading (C), were used with their levels (Table 4).[30]

The most suitable orthogonal array for experimentation is L16 array as shown in Table 5. Therefore, a total 16 experiments are to be carried out. Whereas, the full factorial experimental design requires $3^4 = 81$ different experiments to evaluate the influencing factors. Results of these experiments are used to analyze the data and predict the quality of components produced. Table 5 presents the required experiments to optimize the batch system which were designed using Taguchi method. Initially, we carried out a model reaction to optimize the reaction conditions including solvent, base and catalyst loading. In each run, commonly used bases and solvents, including organic and inorganic bases and polar protic solvents to non-polar aprotic solvents were tested. Also, different amounts of catalyst loadings (mol %) were used

TABLE 4 Controllable factors and their levels

Factor	Description	Level 1	Level 2	Level 3	Level 4
B	Base	K_2CO_3	K_3PO_4	NaOAC	NEt_3
S	Solvent	DMF	DMF/Water	Ethanol	Water
C	Catalyst (mol %)	0.01	0.001	0.005	0.0005

TABLE 5 L_{16} orthogonal array and experimental results

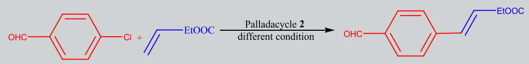

	Factor			Yield (%)	S/N ratio
Run	B	S	C		
1	K_2CO_3	DMF	0.0050	88	38.8897
2	K_3PO_4	DMF	0.0100	73	37.2665
3	NaOAC	DMF	0.0010	60	35.5630
4	NEt_3	DMF	0.0005	43	32.6694
5	K_2CO_3	DMF/Water	0.0010	68	36.6502
6	K_3PO_4	DMF/Water	0.0005	63	35.9868
7	NaOAC	DMF/Water	0.0050	60	35.5630
8	NEt_3	DMF/Water	0.0100	53	34.4855
9	K_2CO_3	Ethanol	0.0005	55	34.8073
10	K_3PO_4	Ethanol	0.0010	50	33.9794
11	NaOAC	Ethanol	0.0100	67	36.5215
12	NEt_3	Ethanol	0.0050	60	35.5630
13	K_2CO_3	Water	0.0100	53	34.4855
14	K_3PO_4	Water	0.0050	58	35.2686
15	NaOAC	Water	0.0005	45	33.0643
16	NEt_3	Water	0.0010	48	33.6248

in different temperatures to find optimum reaction conditions. All experiments were repeated, and the yield percentage of reaction was calculated for each experiment.[31]

We applied the signal-to-noise (S/N) ratio to evaluate the experimental data, the S/N ratio analysis chosen was the larger-the-better.[32] According the values of mean S/N ratio is shown in Table 5 and the optimum level of each factor was determined from the highest value of S/N ratio revealed in Figure 4. The optimum condition was found to be base: K_2CO_3, K_3PO_4, solvent: DMF, DMF/Water and catalyst loading (mol %): 0.005, 0.01.

Analysis of variance (ANOVA) is used to evaluate the response magnitude in (%) of each parameter in the orthogonal experiment. To conclude the optimum conditions for yield of experiments, we used the relationship between each parameter and their percentage contribution $\rho$and the analysis of variance (ANOVA).[33–35] F-Statistics also illustrates the significance of each factor on the response quality.

The contribution percentage of each factor was shown in Figure 5 while Table 6 shows the ANOVA results obtained from the experimental data; the factors with highest F-value have highest contribution percentage on the yield. Based on Table 6, it is clear that all three factors make an equally important contribution to the yield from the Mizoroki-Heck coupling reaction. A comparison of the experimental and the predicted yield of the reaction

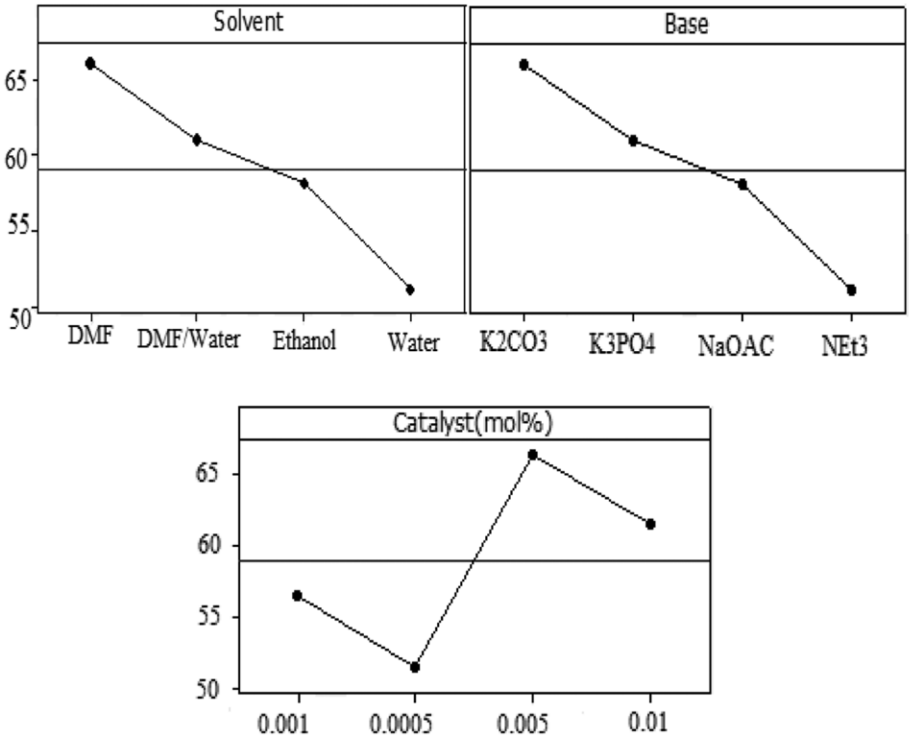

FIGURE 4 Main effect of each factor by S/N ratios

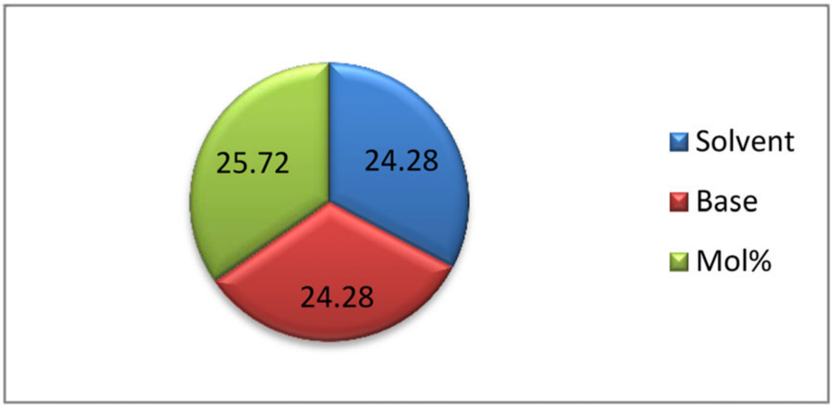

FIGURE 5 Contribution percentage of factors for yield of Suzuki coupling reaction

TABLE 6 Results of the analysis of variance (ANOVA)

Source	DF[a]	Seq. SS[b]	Adj. SS[c]	Adj. MS[d]	F[e]	ρ(%)
S	3	472	472	157.333	*	24.28
B	3	472	472	157.333	*	24.28
C	3	500	500	166.667	*	25.72
Error	3	0	0	0.000		
Total	15	1944				

[a] DF: degree of freedom.

[b] Seq.SS: sequential sum of squares.

[c] Adj.SS: adjusted sum of squares.

[d] Adj.MS: adjusted mean of squares.

[e] F: variance ratio.

have shown in Figure 6 and the variation of the mean yield values against various extraction parameters shown in Figure 7.

The surface plots shown in Figure 8 helps to better display the effects of the experimental factors on the percentage yield. The effects of solvent and base, as shown in Figure 8a, indicate that polar solvents such as DMF and DMF/Water were more efficient in increasing the yield of the products, to 88%. However, the reactions in ethanol and water did not proceed even after prolonged stirring at reflux temperature, probably due to the low solubility of the complexes in this protic solvent. The effect of different mineral bases on this reaction was investigated by using the coupling of p-CHO-Ph-Cl with ethyl acrylate

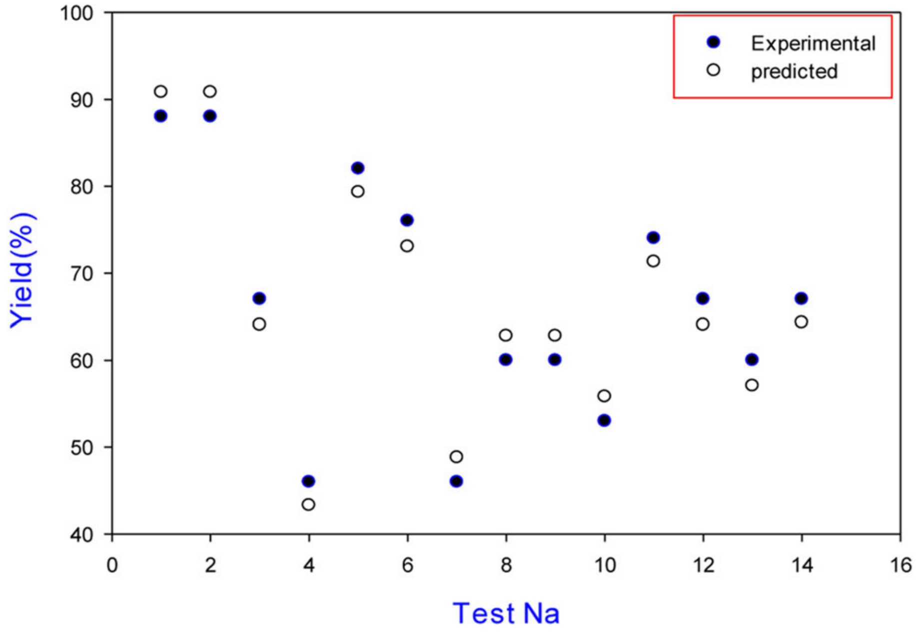

FIGURE 6 Comparison of experimental and predicted yield of reaction

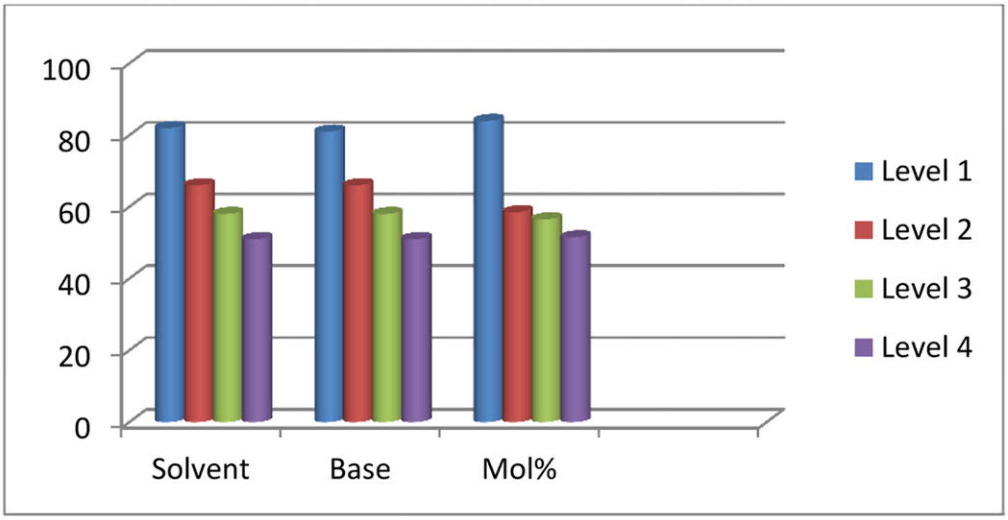

FIGURE 7 The response graph illustrates the variation of the mean yield values plotted against various extraction parameters

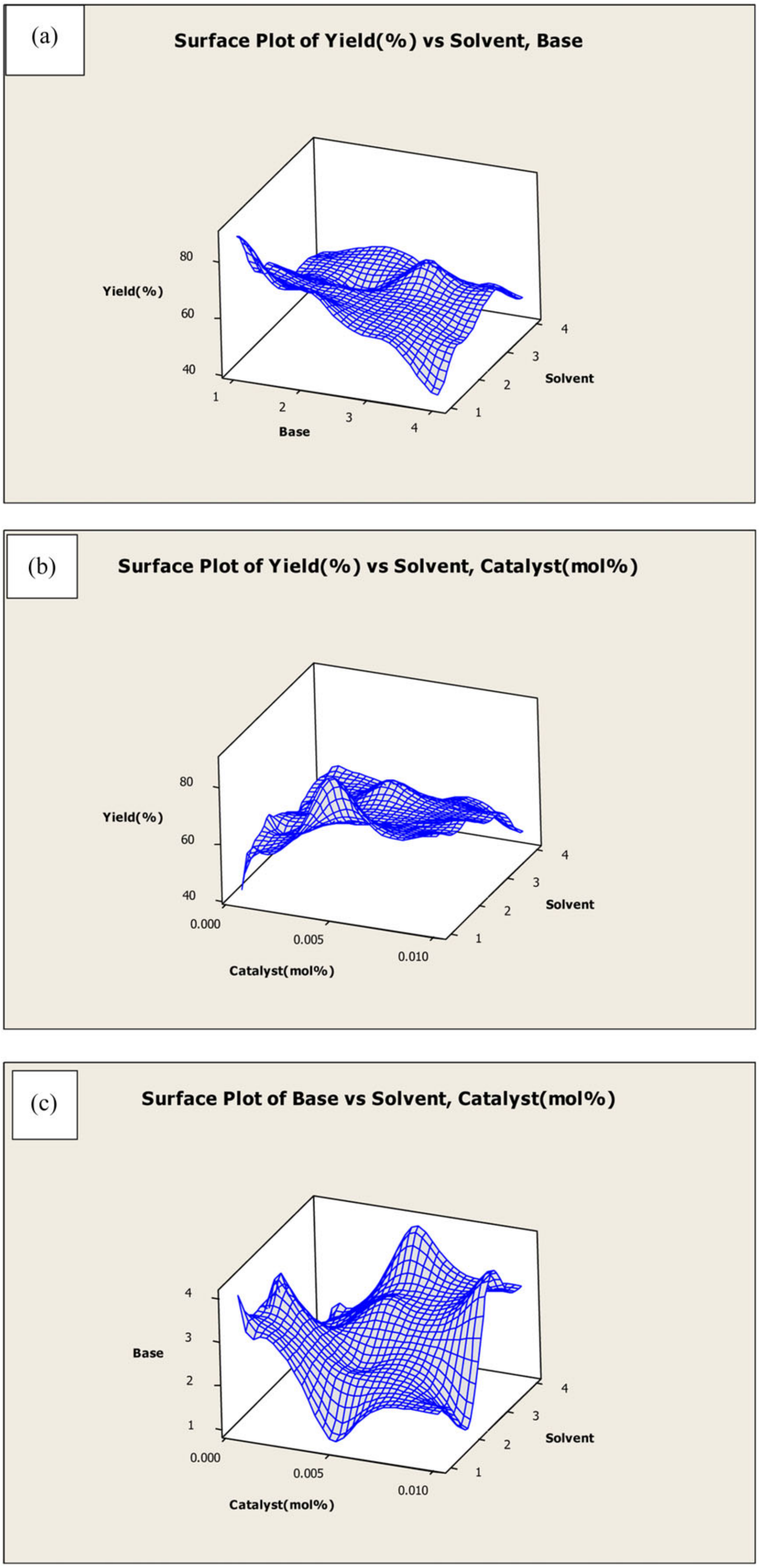

FIGURE 8 Response surface plots for the interaction between factors

TABLE 7 Mizoroki-Heck coupling reaction of aryl chlorides catalyzed by complexes **1** and **2**[a]

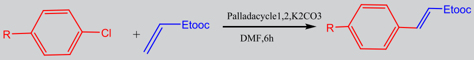

Entry	R	Catalyst	Product	Yield (%)[b]
1	CH_3	**1**	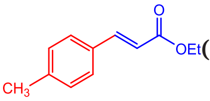 **(5a)**	84
2	CH_3	**2**		88
3	CHO	**1**	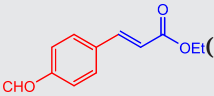 **(5b)**	95
4	CHO	**2**		98
5	NO_2	**1**	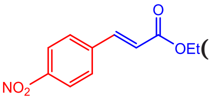 **(5c)**	93
6	NO_2	**2**		95
7	H	**1**	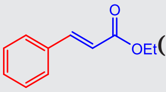 **(5d)**	84
8	H	**2**		88
9	$COCH_3$	**1**	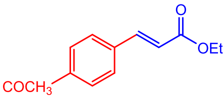 **(5e)**	88
10	$COCH_3$	**2**		90

[a] Reaction conditions for Mizoroki-Heck coupling reaction: aryl chloride (0.5 mmol), olefin (0.75 mmol), K_2CO_3 (1 mmol), DMF (2 ml), catalyst **1**and **2** (0.005 mmol), in air.

[b] Isolated yield.

as a test case. K_2CO_3 and K_3PO_4 were the best choice of base and the yield of product could be increased to 88%. The interaction surface plot of the catalyst loading (mol%) and solvent, as shown in Figure 8b indicate that the percentage yield is higher in DMF and DMF/Water, and with a catalyst loading (mol%) of 0.005. The effects of solvent, base and catalyst loading (mol %), as shown in Figure 6c, and confirm above results.

3.4.2 | Mizoroki-heck coupling reaction of functionalized aryl chlorides

Using the optimized reaction conditions, complexes **1** and **2** were applied in the reaction of various functionalized aryl chlorides bearing both electron-donating to electron-withdrawing groups with olefin. Aryl chlorides were converted into the corresponding coupled products in high to excellent yields (Table 7).

A comparison between the catalytic activities of presented complexes and other Pd catalysts having different ancillary ligands in Suzuki-Miyaura reaction was carried out. The results indicated that the differences in catalytic behavior demonstrated in Table 8 should be ascribed not only to the differences in the experimental conditions (e.g. effects of solvent, base, and catalyst loading), but mainly attributed to the characteristic differences in the Pd content. The donor atoms of ligand have substantial effect on stabilization and consequently performance of Pd catalyst and the ligand-controlling conditions is clearly obvious in such catalytic reactions carried out under similar experimental conditions. Compound 2 seems to give the best results in accordance with Table 8.

4 | CONCLUSIONS

The present study describes the synthesis and characterization of new diphosphinium salt **S** diphosphine ylide **Y**^{1} and complexes **1** and **2** derived from $PdBr_2COD$ and bifunctionalized phosphorus ylides (**Y**^{1} and **Y**^{2}) by simple and convenient synthetic methods in satisfactory yields. These compounds were characterized using FT-IR, and NMR (^{1}H, ^{13}C and ^{31}P) analyses as well as X-ray structural analyses. The catalytic activity of complexes **1** and

TABLE 8 Comparison of Mizoroki-Heck coupling reaction of *p*-nitrochlorobenzene and ethyl acrylate using palladacycle **2** and other catalytic system

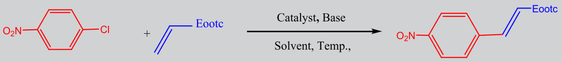

Entry	Pd source	Catalyst loading (mmol)	Condition	Yield (%)	Ref.
1	Pd (II)-NHC complexes	0.5	K_3PO_4, DMA, 110 °C, 5 hr	52–90	36
2	[(C3H5)PdCl]2-N,N,N′,N′-tetra (diphenylphosphinomethyl)-1,2-ethylenediamine	0.1	$NaHCO_3$, DMF: DMA,120 °C, 20 hr	96	37
3	Oxime-Derived Palladium Complexes	0.5	K_2CO_3, DMF, 130 °C, 5 hr	77	38
4	$PdCl_2(MeCN)_2$	0.05	K_3PO_4, DMF, 130 °C, 24 hr	69	39
5	P, C-chelated phosphorus ylide Pd (II)	0.005	K_2CO_3, DMF, 130 °C, 6 hr	95	This work

2 toward Mizoroki-Heck cross-coupling reaction has been investigated while the Taguchi method has been used to optimize the yield of the products of the Mizoroki-Heck coupling reaction. The results also indicate that utilization of the Taguchi method gives a suitable approach for optimization of the yield of the Mizoroki-Heck coupling. The effect of each factor was estimated using individual contributions as response functions. The results of ANOVA showed that the all factors (solvent, base and catalyst (mol%) have significant effect on the yield and have highest F and high contribution percentage on the yield of Mizoroki-Heck coupling process.

ACKNOWLEDGEMENTS

Funding of our research from the Bu-Ali Sina University is gratefully acknowledged.

SUPPLEMENTARY MATERIAL

Physical measurements and selected ^{31}P, ^{13}C and ^{1}H NMR spectra of some compounds can be found in the online version. CCDC 1431939 and 1812607 contains the supplementary crystallographic data for the complexes **1** and **2**, respectively. These data can be obtained free of charge via www.ccdc.cam.ac.uk/data_request/cif or from the Cambridge Crystallographic Data Center, 12, Union Road, Cambridge CB2 1EZ, UK. Tel.: +44 0 1223 762911; or deposit@ccdc.cam.ac.uk.

ORCID

Seyyed Javad Sabounchei https://orcid.org/0000-0001-9000-5304

REFERENCES

[1] E. C. Spencer, M. B. Mariyatra, J. A. K. Howard, A. M. Kenwrigh, K. J. Panchanatheswaran, *Organomet. Chem.* **2007**, *5*, 1081.

[2] S. J. Sabounchei, M. Ahmadi, F. AkhlaghiBagherjeri, H. R. Khavasi, *J. Chem. Sci.* **2013**, *3*, 653.

[3] S. J. Sabounchei, A. Hashemi, A. Yousefi, P. Gohari Derakhshandeh, R. Karamian, M. Asadbegy, K. Van Hecke, *Polyhedron* **2017**, *135*, 1.

[4] D. Aguilar, M. A. Aragues, R. Bielsa, E. Serrano, T. Soler, L. R. Navarro, E. P. Urriolabeitia, *J. Organomet. Chem.* **2008**, *3*, 417.

[5] A. Spannenberg, W. Baumann, U. Rosenthal, *Organometallics* **2000**, *19*, 3991.

[6] S. J. Sabounchei, M. Hosseinzadeh, S. Salehzadeh, F. Maleki, R. W. Gable, *Inorg. Chem. Front.* **2017**, *2017*, 4.

[7] E. C. Spencer, B. Kalyanasundari, M. Baby Mariyatra, J. A. K. Howard, K. Panchanatheswaran, *Inorg. Chim. Acta* **2006**, *359*, 35.

[8] R. E. Cramer, S. Roth, F. Edelmann, M. A. Bruck, K. C. Cohn, J. W. Gilje, *Organometallics* **1989**, *8*, 1192.

[9] M. M. Ebrahim, H. Stoeckli-Evans, K. Panchanatheswaran, *Polyhedron* **2007**, *26*, 3491.

[10] E. C. Spencer, M. B. Mariyatra, J. A. K. Howard, A. M. Kenwright, K. Panchanatheswaran, *J. Organomet. Chem.* **2007**, *692*, 1081.

[11] S. J. Sabounchei, M. Panahimehr, M. Ahmadi, Z. Nasri, H. R. Khavasi, *J. Organomet. Chem.* **2013**, *723*, 207.

[12] S. J. Sabounchei, M. Panahimehr, M. Ahmadi, F. Akhlaghia, C. Boscovic, *C. R. Chim.* **2014**, *17*, 81.

[13] S. J. Sabounchei, M. Ahmadi, Z. Nasri, E. Shams, S. Salehzadeh, Y. Gholiee, R. Karamian, M. Asadbegy, S. Samiee, *C. R. Chim.* **2013**, *16*, 159.

[14] B. L. Shaw, S. D. Perera, *Chem. Commun.* **1998**, *17*, 1863.

[15] L. D. Deborah, D. K. B. Maarten, P. F. Gino, G. V. Johannes, W. N. M. Piet, C. J. K. Paul, *Eur. J. Inorg. Chem.* **2012**, *10*, 1660.

[16] A. Ghorbani-Choghamarani, A. Naghipour, H. Babaee, B. Notash, *Polyhedron* **2016**, *119*, 517.

[17] S. J. Sabounchei, M. Ahmadi, *Cat. Com.* **2013**, *37*, 114.

[18] S. J. Sabounchei, A. Sedghi, A. Hashemi, M. Hosseinzadeh, M. Bayat, R. W. Gable, *Appl. Organomet. Chem.* **2017**, *31*, 3850.

[19] S. J. Sabounchei, A. Hashemi, M. Hosseinzadeh, S. Salehzadeh, F. Maleki, *Catal. Lett.* **2017**, *147*, 2319.

[20] H. Yuan Yen, J. Yan Li, *J. Environ. Manage.* **2015**, *161*, 344.

[21] D. Drew, J. R. Doyle, A. G. Shaver, *Inorg. Synth.* **1972**, *13*, 47.

[22] O. V. Dolomanov, L. J. Bourhis, R. W. Grosse-Kunstleve, P. D. Adams, R. J. Gildea, J. A. K. Howard, H. Puschmann, *J. Appl. Crystallogr.* **2011**, *44*, 1259.

[23] G. M. Sheldrick, *Acta Crystallogr. A* **2015**, *C71*, 3.

[24] G. M. Sheldrick, *Acta Crystallogr.* **2015**, *A71*, 3.

[25] M. Carbo, N. Marin, R. Navarro, T. Soler, E. P. Urriolabeitia, *Eur. J. Inorg. Chem.* **2006**, *2006*, 4629.

[26] S. J. Sabounchei, S. Samiee, D. Nematollahi, A. Naghipour, D. M. Morales, *Inorg. Chim. Acta* **2010**, *363*, 3973.

[27] S. J. Sabounchei, H. Nemattalab, H. R. Khavasi, *X-Ray Struct. Anal. Online* **2010**, *26*, 35.

[28] P. J. Ross, *Taguchi techniques for quality engineering*, McGraw-Hill, Singapore **1996**.

[29] M. A. Schoonen, J. M. T. Schoonen, *J. Colloid Interface Sci.* **2014**, *422*, 1.

[30] M. P. Elizalde-González, L. E. Garcia-Diaz, *Chem. Eng. J.* **2010**, *163*, 55.

[31] J. Zolgharnein, N. Asanjarani, T. Shariatmanesh, *Int. Biodeterior. Biodegrad.* **2013**, *85*, 66.

[32] B. Ramavandi, G. Asgari, J. Faradmal, S. Sahebi, B. Roshani, *Korean J. Chem. Eng.* **2014**, *31*, 2207.

[33] S. Athreya, Y. D. Venkatesh, *Int. Refereed J. Eng. Sci.* **2012**, *1*, 13.

[34] C. S. Chou, R. Y. Yang, J. H. Chen, S. W. Chou, *Powder Technol.* **2010**, *199*, 264.

[35] N. J. Cox, J. Warburton, A. Armstrong, V. J. Holliday, *Earth Surf. Process. Landf.* **2008**, *33*, 25.

[36] K. R. Balinge, P. R. Bhagat, *C. R. Chim.* **2017**, *20*, 773.

[37] X.-J. Yu, R. Zhou, Y. Zhang, H. Yan Fu, R. Xiang Li, H. Chen, X. Jun Li, *Cat. Com.* **2010**, *12*, 222.

[38] D. A. Alonso, C. Najera, M. C. Pacheco, *Adv. Synth. Catal.* **2002**, *67*, 5588.

[39] T. Mino, Y. Shirae, Y. Sasai, M. Sakamoto, T. Fujita, *J. Org. Chem.* **2006**, *71*, 6834.

SUPPORTING INFORMATION

Additional supporting information may be found online in the Supporting Information section at the end of the article.

How to cite this article: Sabounchei SJ, Badpa K, Hashemi A, Moniriyan F, Gable RW. Spectral and crystallography studies of new palladacycle complexes with P,C- and C,C-donor ligands; Application of (OAL16) to optimizing the yield of Mizoroki-Heck reaction. *Appl Organometal Chem*. 2019;e4882. https://doi.org/10.1002/aoc.4882